ARTICLES

nature structural & molecular biology

Communication between ClpX and ClpP during substrate processing and degradation

Shilpa A Joshi[1], Greg L Hersch[1], Tania A Baker[1,2] & Robert T Sauer[1]

In the ClpXP compartmental protease, ring hexamers of the AAA+ ClpX ATPase bind, denature and then translocate protein substrates into the degradation chamber of the double-ring $ClpP_{14}$ peptidase. A key question is the extent to which functional communication between ClpX and ClpP occurs and is regulated during substrate processing. Here, we show that ClpX-ClpP affinity varies with the protein-processing task of ClpX and with the catalytic engagement of the active sites of ClpP. Functional communication between symmetry-mismatched ClpXP rings depends on the ATPase activity of ClpX and seems to be transmitted through structural changes in its IGF loops, which contact ClpP. A conserved arginine in the sensor II helix of ClpX links the nucleotide state of ClpX to the binding of ClpP and protein substrates. A simple model explains the observed relationships between ATP binding, ATP hydrolysis and functional interactions between ClpX, protein substrates and ClpP.

AAA+ ATPases function as essential components of energy-dependent compartmental proteases in all biological kingdoms[1]. For example, the 19S portion of the eukaryotic proteasome consists predominantly of AAA ATPases, which help recognize and translocate substrates to an associated 20S protease[2]. In bacteria, the ClpXP and ClpAP proteases consist of either the ClpX or ClpA ATPase and the ClpP peptidase, and the HslUV protease consists of the HslU ATPase and the HslV peptidase[1,3,4]. In each of these energy-dependent proteases, the active sites for polypeptide cleavage are sequestered in a degradation chamber formed by a multisubunit barrel-shaped complex[5–14]. Entry portals that are too small to admit native proteins provide access to this chamber. The ATPases of compartmentalized proteases from bacteria form ring hexamers that bind appropriate protein substrates, unfold these molecules and translocate them through a central protein-processing pore and into the peptidase chamber for degradation[1,3,4]. The interaction of ATP and its γ-phosphate with these proteolytic ATPases is mediated in part by evolutionarily conserved sensor I and II sequence motifs[15,16].

One key question for all energy-dependent proteases is how interactions between the ATPase and the peptidase coordinate substrate processing and degradation. For HslUV, the peptidase and ATPase are both six-fold symmetric, and structures of the complex in different nucleotide-bound states are known[9,11,13,17,18]. Nucleotide binding modulates the size of the protein-processing pore and the entry portal and also alters contacts between HslU and HslV, propagating structural changes to the peptidase active sites and mediating communication between the ATPase and peptidase[11,17–22].

For ClpXP (**Fig. 1**) and ClpAP[7,8,23–25], docking of the ATPase and peptidase involves a symmetry mismatch between a hexameric ATPase ring and a heptameric ClpP ring. Although high-resolution structures of these protease complexes have not been solved, flexible surface loops in both ClpX and ClpA, which contain an IGF or IGL motif, have been implicated in ClpP binding[26–29]. Despite the symmetry mismatch, coordination between the activities of the six-fold symmetric ATPase and seven-fold symmetric peptidase must occur, because binding of ClpA activates ClpP peptidase activity[30], proteins trapped in the degradation chamber of inactive ClpP can be released in a reaction that depends upon ATP hydrolysis by ClpX[31], and the ATPase activities of ClpA and ClpX are depressed upon binding to ClpP[26,32].

To probe functional communication between the ClpX and ClpP enzymes of *Escherichia coli*, we used changes in ATPase activity to monitor and quantify the strength of the ClpX-ClpP interaction. We find that ClpP binds most tightly to ClpX when the ATPase is denaturing protein substrates, less tightly during translocation of substrates and least tightly in the absence of substrates. ClpX can also detect the catalytic status of the ClpP active sites, as shown by a marked increase in affinity when the active site serines of ClpP are modified. ClpP binding suppresses the protein-unfolding defects of ClpX variants with mutations at an intersubunit interface, but rescue occurs at the expense of binding affinity and reverses the response to substrate processing. This result suggests that interactions between subunits in wild-type ClpX have an important role in the unfolding of protein substrates by preventing quaternary distortions in ClpX that block substrate denaturation and weaken ClpP binding. Finally, we demonstrate that a conserved arginine in the sensor II motif of ClpX links ATP binding to conformational changes required for binding of ClpP and protein substrate.

RESULTS

Substrate design

Protein substrates had C-terminal ssrA tags to target them to ClpX[33]. Unfolding of GFP-ssrA by ClpX or degradation by ClpXP results in

[1]Department of Biology, Massachusetts Institute of Technology, and [2]Howard Hughes Medical Institute, 77 Massachusetts Avenue, Cambridge, Massachusetts 02139, USA. Correspondence should be addressed to R.T.S. (bobsauer@mit.edu).

Published online 4 April 2004; doi:10.1038/nsmb752

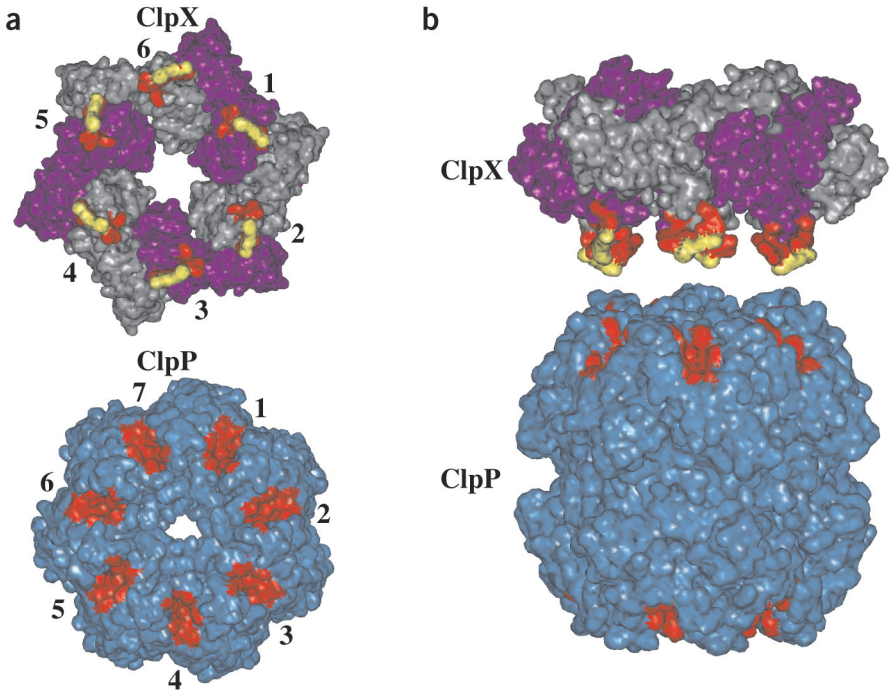

Figure 1 Symmetry mismatch between ClpX and ClpP. (**a**) Axial views of the interaction surfaces of ClpX and ClpP[7,29]. Subunits in $ClpX_6$ are purple or gray, whereas subunits in the visible heptameric ring of $ClpP_{14}$ are blue. Part of the ClpX loop that mediates ClpP binding is red, and the signature tripeptide at its tip is yellow. Hydrophobic clefts in ClpP are also red. (**b**) Side view showing how the IGF loops of ClpX might align with the hydrophobic clefts of ClpP.

loss of fluorescence[31,34]. Unlabeled and ^{35}S-labeled variants of the human titin-I27-ssrA protein were degraded by ClpXP either as native proteins or as denatured, carboxymethylated (CM) molecules[35].

ClpP interaction requires more than two IGF loops

The IGF loop (residues 264–278) of *E. coli* ClpX mediates binding to ClpP[26,27]. We constructed and purified ClpX loopless, a variant in which this loop was replaced with a short linker. As expected, ClpX loopless did not support degradation of an ssrA-tagged substrate in the presence of ClpP (**Fig. 2a**) and did not bind His_6-ClpP in Ni^{2+}-NTA pull-down assays (data not shown). ClpX loopless was, however, as active as wild-type ClpX in unfolding GFP-ssrA, as monitored by loss of native GFP fluorescence (**Fig. 2b**). Moreover, ClpX loopless formed stable ternary complexes with GFP-ssrA and the delivery protein SspB during gel filtration in the presence of ATPγS (**Fig. 2c**). These mutant complexes chromatographed at the same position as wild-type complexes, suggesting that ClpX loopless, like ClpX, is hexameric under these conditions[36]. We conclude that ClpX loopless fails to interact with ClpP but otherwise assembles normally and is active in binding and denaturing ssrA-tagged substrates.

It is not known how many IGF loops in a ClpX hexamer (a trimer of stable dimers[37]) are required for functional collaboration with ClpP. An IGF-loop peptide bound ClpP very weakly ($K_d > 200$ μM; data not shown), suggesting that stable ClpP binding requires that several IGF loops be present and/or that the loop be held in a specific conformation by ClpX. To test the activity of hexamers containing mixtures of wild-type and loopless dimers, we added ClpX loopless to wild-type ClpX and assayed degradation of an ssrA-tagged substrate in the presence of excess ClpP. A modest excess of ClpX loopless inhibited degradation (**Fig. 2d**), with the data fitting a model in which hexamers with only one wild-type dimer have <1% activity, those with two wild-type dimers are ~60% active, and mixing of wild-type and mutant dimers is unbiased. Pull-down experiments confirmed that wild-type and loopless ClpX form mixed multimers (data not shown). We conclude that functional interactions between ClpX and ClpP require IGF loops in at least two of the dimers that comprise the ClpX hexamer.

ATPase assay for ClpX-ClpP affinity

ClpP binding decreases the rate of ATP hydrolysis by ClpX[26]. ATP turnover by 50 nM $ClpX_6$ or $ClpX_6$ loopless was assayed in the presence of $ClpP_{14}$ at concentrations ranging from 0 to 2.5 μM. No

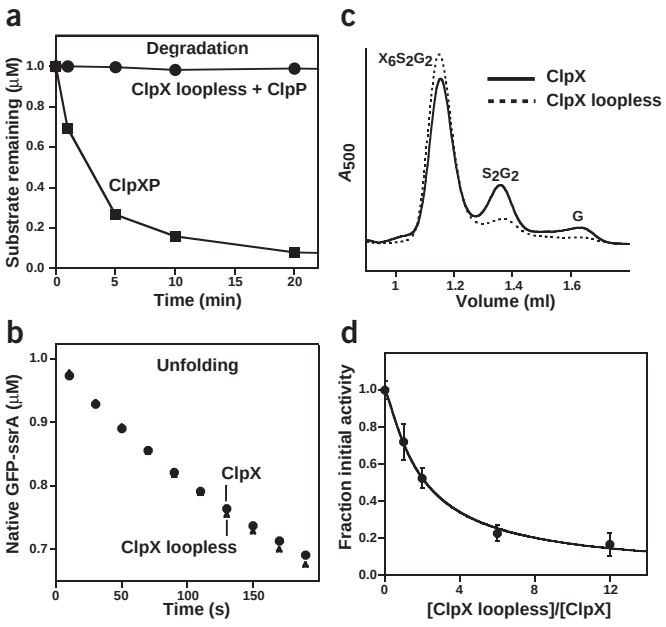

Figure 2 Properties of ClpX loopless. (**a**) $ClpX_6$ loopless (100 nM) did not support degradation of CM-titin-V13P-ssrA (1 μM) in the presence of $ClpP_{14}$ (300 nM), whereas wild-type ClpX mediated efficient degradation under these conditions. (**b**) GFP-ssrA (1 μM) in the presence of $SspB_2$ (1 μM) was unfolded at essentially the same rate by $ClpX_6$ or $ClpX_6$ loopless (300 nM), as assayed by loss of native GFP-ssrA fluorescence. (**c**) ClpX loopless forms stable ternary complexes. $ClpX_6$ or $ClpX_6$ loopless (6 μM), $SspB_2$ (3 μM), GFP-ssrA (6 μM) and ATPγS (5 mM) were chromatographed on a gel-filtration column, and the elution position of GFP-ssrA was monitored by A_{500}. Positions of the ternary complex ($X_6S_2G_2$), binary complex of SspB and GFP-ssrA (S_2G_2), and free GFP-ssrA (G) are shown. (**d**) Degradation of titin-V4A-ssrA (5 μM) by wild-type ClpXP (100 nM $ClpX_6$; 2 μM $ClpP_{14}$) was inhibited by addition of ClpX loopless. The solid line is a fit to equation (3) (see Methods) with a bias factor of 0.99, an A_{21} value of 0.63 and an A_{12} value of 0.003.

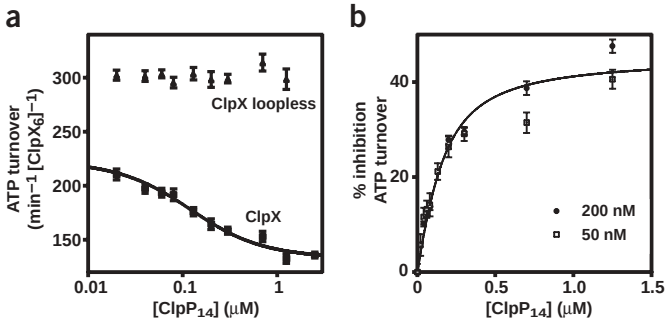

Figure 3 An assay for ClpX-ClpP interaction in solution. (**a**) Changes in the ATP hydrolysis rate of 50 nM $ClpX_6$ or $ClpX_6$ loopless as a function of ClpP concentration. Data in linear form were fitted to equation (1) and then plotted in semilog form. (**b**) Percentage inhibition of ATP turnover as a function of ClpP concentration with two different $ClpX_6$ concentrations. The fitted line is that expected for a 1:1 binding reaction (equation 1) with an apparent affinity of 92 ± 17 nM.

substantial changes in ATPase activity were observed for the ClpX loopless control. In contrast, for wild-type ClpX, changes in rate fit well to a simple binding isotherm (**Fig. 3a**). These experiments confirm the importance of the IGF loop in binding ClpP and indicate that the changes in ATP hydrolysis when ClpP binds ClpX are mediated by the same region of the protein that permits collaboration in protein degradation. Assays done with 200 nM $ClpX_6$ gave similar results, with the combined data obtained for the two ClpX concentrations fitting a 1:1 binding model in which $ClpX_6$ and $ClpP_{14}$ interact with an apparent equilibrium dissociation constant (K_{app}) of 92 ± 17 nM (**Fig. 3b**). These results indicate that ClpX hexamers do not dissociate significantly in the concentration range of 50–200 nM. Nevertheless, it is important to note that K_{app} reflects a population-weighted average of the K_d values of ClpP for the ClpX hexamer in each of its different enzymatic and conformational states as it passes through its cycles of ATP hydrolysis and coupled conformational changes.

Substrate processing strengthens ClpX-ClpP affinity

Studies using titin-ssrA substrates with a range of stabilities showed that ClpX denatures these molecules at different rates but translocates the denatured proteins to ClpP at the same rate[35]. Hence, we reasoned that assaying ClpX-ClpP affinity during degradation of these titin substrates should reveal whether protein denaturation and translocation affect this interaction. ATPase assays were used to monitor ClpP affinity in the presence of concentrations of titin-ssrA substrates that ensured ~90% saturation of ClpX. When ClpP was titrated against ClpX in the presence of the most stable native substrate, wild-type titin-ssrA, K_{app} was 19 ± 5 nM, roughly five-fold lower than the value in the absence of substrate (**Figs. 3a** and **4a**). In the presence of less stable native variants, K_{app} values were 27 ± 3 nM (V15P) and 53 ± 9 nM (V13P). When a denatured titin substrate (CM-V13P) was present, K_{app} was 78 ± 9 nM. With other denatured substrates (CM-titin; CM-V15P), K_{app} values were within experimental error of the CM-V13P value (data not shown). These results show that the apparent affinity for ClpP is stronger when ClpX is processing titin-ssrA substrates, with the strongest binding observed for native substrates that are denatured most slowly.

K_{app} for ClpX-ClpP binding in the presence of various titin-ssrA substrates was linearly correlated ($R = 0.99$) with the rate constants for degradation (**Fig. 4b**). Although more complicated models are possible, this relationship could be explained simply by a situation in which ClpX has one affinity for ClpP while denaturing titin-ssrA substrates and a different, weaker affinity while translocating these substrates. Indeed, the linear fit (**Fig. 4b**) represents a model in which K_{app} is 16 nM during denaturation and 70 nM during translocation (see Methods). These results suggest a mechanism by which ClpP can detect the protein-processing task in which ClpX is engaged. The ClpX-ClpP affinities were also well correlated with the rates of ATP turnover by ClpXP and ClpX in the presence of the titin-ssrA substrates (**Fig. 4c**). These observations lead us to suggest that the ATPase rate of ClpX during substrate processing, which depends on the average time required for denaturation and translocation, controls its apparent affinity for ClpP.

Active site communication between ClpP and ClpX

If ClpP can detect whether ClpX is processing protein substrates, then ClpX may be able to detect whether ClpP is degrading substrates. To address this possibility, we used DFP-ClpP, a variant in which the active site serines (Ser97) were covalently modified by reaction with di-isopropyl-fluorophosphate (DFP)[31]. Although DFP-ClpP is inactive in degradation, the modification mimics the acyl-enzyme intermediate in peptide bond hydrolysis. Moreover, a DFP oxygen binds in the oxyanion hole of the active site, mimicking the carbonyl oxygen of

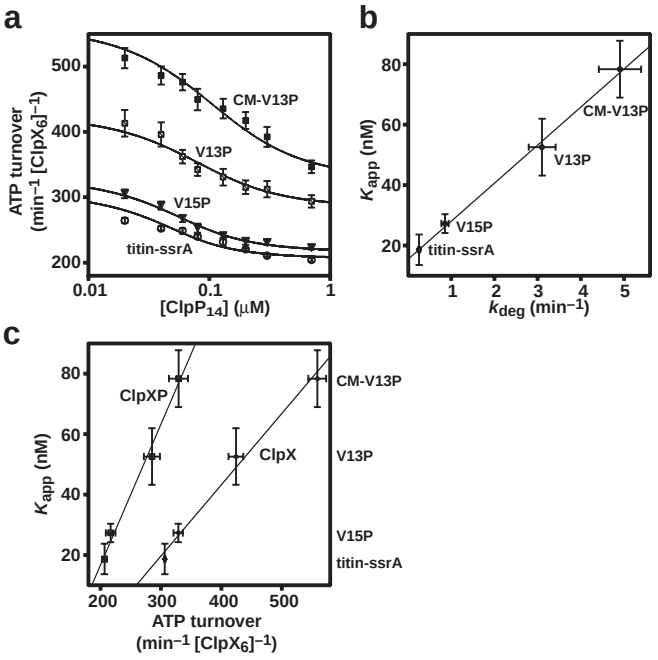

Figure 4 ClpX-ClpP affinity changes in an ATPase-dependent manner during substrate denaturation and translocation. (**a**) Binding of ClpP to 50 nM $ClpX_6$ in the presence of 15 μM concentrations of four variants of titin-ssrA. The fits represent K_{app} values of 19 ± 5 nM for wild-type titin-I27-ssrA, 27 ± 3 nM for the native V15P mutant, 53 ± 9 nM for the native V13P variant and 78 ± 9 nM for the denatured CM-V13P protein. (**b**) K_{app} values for the ClpX-ClpP interaction in the presence of titin-ssrA substrates vary linearly with the rate constant for ClpXP degradation of these substrates[35]. The line is a fit to equation (2) (see Methods), with affinities of 16 and 70 nM, respectively, when ClpXP is denaturing or translocating titin-ssrA substrates. (**c**) K_{app} for the ClpX-ClpP interaction correlates linearly ($R = 0.99$) with the ATPase rates of ClpXP and ClpX during the processing of different titin-ssrA substrates. ClpXP ATPase rates are values obtained with saturating concentrations of ClpP.

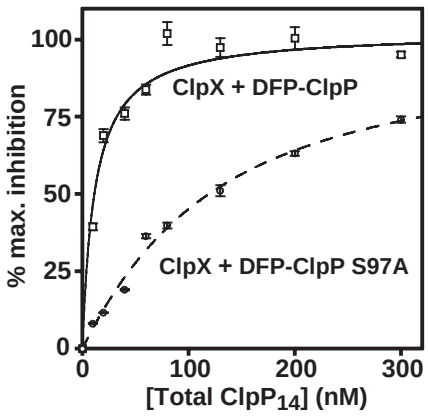

Figure 5 Modification of the ClpP active sites strengthens ClpX binding. DFP-ClpP bound tightly to 50 nM $ClpX_6$, as assayed by changes in ATP hydrolysis. $ClpP_{14}$ can bind two ClpX hexamers and, at half-maximal binding, the total concentration of DFP-$ClpP_{14}$ was ~15 nM and the concentration of bound $ClpX_6$ was 25 nM. Although an accurate K_{app} cannot be determined from these data, the upper limit for this constant is ~5 nM. K_{app} for the interaction of ClpX with DFP-treated ClpP S97A (94 nM) was similar to that for wild-type ClpP, confirming that the tight binding of DFP-ClpP results from modification of the active site Ser97 side chain.

a peptide substrate[7]. DFP-ClpP bound ClpX so strongly that the bound and total concentrations of ClpX were essentially the same (**Fig. 5**). This 'stoichiometric binding' indicates that the affinity constant is ≤5 nM. Hence, ClpX seems to be capable of sensing whether the ClpP active sites are engaged with substrate. To ensure that the tighter ClpX binding observed for DFP-ClpP was caused by modification of the active site Ser97, we assayed binding of a ClpP S97A mutant after treatment with DFP[38]. DFP-treated ClpP S97A bound ClpX similarly to wild-type ClpP and much more weakly than DFP-ClpP (**Fig. 5**). We conclude that the strong ClpX binding observed for DFP-ClpP results from acylation of the active site serines and/or from concomitant substrate-like interactions of the covalent modification.

ClpP rescues the unfolding defects of ClpX mutants

Mutations in the C-terminal portion of the ClpX sensor II helix, which forms part of the interface between the C domain of one subunit and the ATPase domain of an adjacent subunit, cause defects in substrate unfolding but not in substrate binding[39]. Because ClpP binds more tightly when ClpX is denaturing substrates, we reasoned that ClpP binding might suppress the unfolding defects of these sensor II mutants. This result was observed. By themselves, ClpX L381K and ClpX D382K had undetectable activities in unfolding GFP-ssrA (**Fig. 6a**). In the presence of DFP-ClpP, however, the same mutants catalyzed efficient unfolding of GFP-ssrA (**Fig. 6b**). Unmodified ClpP also suppressed the unfolding defects of these sensor II mutants (data not shown). Because DFP-ClpP suppressed most efficiently the unfolding defect of ClpX D382K, we selected this ClpX variant for more detailed studies.

In the absence of substrate, ClpP bound ClpX D382K (K_{app} = 0.12 ± 0.05 μM; **Fig. 6c**) only slightly more weakly than wild-type ClpX. When substrate was present, however, the affinity of ClpP for this mutant was substantially worse. K_{app} was ~20-fold weaker (2.3 ± 0.5 μM) in the presence of the native V13P variant of titin-ssrA and ~10-fold weaker (1.1 ± 0.4 μM) in the presence of denatured CM-titin-ssrA (**Fig. 6d**). Thus, whereas the affinity of ClpP for wild-type ClpX increases during the processing of protein substrates, the opposite is true for the D382K mutant. These data suggest that when ClpX D382K engages a protein substrate, it must assume a conformation poorly suited for binding ClpP and substrate unfolding. Although ClpP can stabilize ClpX D382K in an active conformation, the energy used for this conformational change reduces affinity. Unusually, addition of ClpP to ClpX D382K (**Fig. 6d**) increased the ATP hydrolysis rate in the presence of protein substrates. By contrast, ClpP binding reduced ATPase activity for ClpX D382K without substrate (**Fig. 6c**) and for wild-type ClpX under all conditions (**Figs. 3a** and **4a**). These results are consistent with a distorted conformation for complexes between ClpX D382K and substrates.

Nucleotide state of ClpX controls ClpP binding

The experiments just presented suggest that ClpX ATPase activity is linked to interactions with ClpP. In pull-down assays, untagged ClpP bound Ni^{2+}-NTA in the presence of His_6-ClpX and ATPγS but did not bind well when ATP or ADP was present (**Fig. 7a**). Because ATP is hydrolyzed rapidly by ClpX, ClpX•ADP may predominate even with excess ATP if ADP release is slow. By contrast, ATPγS is hydrolyzed slowly by ClpX[40], and thus ClpX•ATPγS is probably the best mimic of the 'ATP' state. ATP binding therefore seems to increase the affinity of ClpX for ClpP. Peptides containing the ssrA degradation tag also bind most tightly to ClpX in the ATP-bound state[36] (D. Wah, Massachusetts Institute of Technology (MIT), personal communication).

To test whether contacts between ClpX and ATP have a role in stabilizing ClpP binding, we constructed and purified a ClpX mutant in

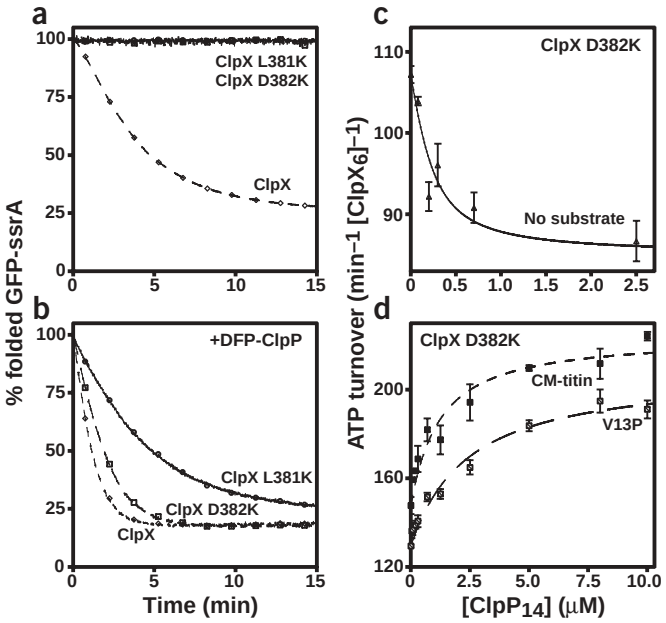

Figure 6 ClpP rescues the unfolding defects of ClpX mutants. (**a**,**b**) The sensor II helix mutants, ClpX D382K and ClpX L381K, fail to unfold GFP-ssrA (310 nM) by themselves (**a**) but unfold this substrate efficiently in the presence of 800 nM DFP-$ClpP_{14}$ (**b**). In these experiments, the concentrations of mutant or wild-type $ClpX_6$ were 260 nM, and 460 nM SspB was present. (**c**,**d**) ClpP binds 200 nM $ClpX_6$ D382K with an apparent affinity of 120 ± 50 nM in the absence of substrate (**c**) but binds more weakly in the presence of a denatured substrate (13.1 μM CM-titin-ssrA; K_{app} = 1.1 ± 0.4 μM) or a native substrate (15 μM titin-V13P-ssrA; K_{app} = 2.3 ± 0.5 μM) (**d**).

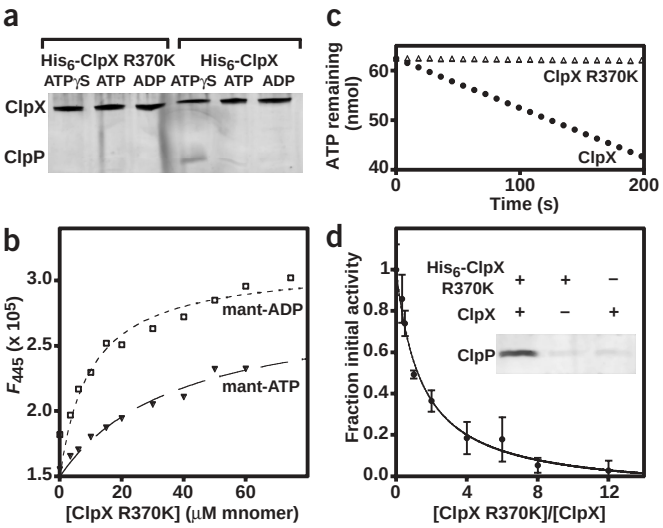

Figure 7 The ATP state of ClpX is required for strong ClpP interactions. (**a**) Untagged ClpP bound Ni^{2+}-NTA in the presence of His_6-ClpX and ATPγS; weak binding was observed with ATP or ADP in some experiments but is not visible here. No binding of ClpP to His_6-ClpX R370K was detected with any nucleotide. (**b**) Binding of ClpX R370K to 1 μM mant-ADP or mant-ATP assayed by changes in fluorescence in the absence of magnesium. The fitted lines are for K_d values of 39 μM (mant-ATP) and 18 μM (mant-ADP). (**c**) $ClpX_6$ R370K (400 nM) hydrolyzed ATP at <1% of the rate of wild-type $ClpX_6$ (400 nM), as determined in a coupled spectrophotometric assay[46]. (**d**) Degradation of GFP-ssrA (7 μM) by wild-type ClpXP (100 nM $ClpX_6$; 2.7 μM $ClpP_{14}$) was inhibited by addition of the ClpX R370K mutant. The solid line is a fit to equation (4) (see Methods) with a bias factor of 0.33. Inset: untagged ClpP binds Ni^{2+}-NTA in the presence of a mixture of His_6-ClpX R370K and untagged wild-type ClpX, but binds much less strongly in the presence of either single species. All pull-down reactions contained ATPγS.

which Arg370 was mutated to lysine. This highly conserved side chain resides in the N-terminal portion of the sensor II helix; the corresponding residue in the crystal structure of *Helicobacter pylori* ClpX (Arg396) is positioned to contact bound nucleotide but is distant from the ClpP binding surface[29]. ClpX R370K purified similarly to wild-type ClpX and bound the fluorescent nucleotides (2′ or 3′)-O-(*N*-methylanthraniloyl)-ATP (mant-ATP; K_d = 39 μM) and mant-ADP (K_d = 18 μM) with affinities within two-fold of those for wild-type ClpX[40] (**Fig. 7b**; data not shown). Moreover, ATPγS and ATP competed equally well for binding of mant-ADP to ClpX R370K (R. Burton, MIT, personal communication). Hence, ClpX R370K shows no marked defect in ATP binding. Nevertheless, this mutant failed to hydrolyze ATP (**Fig. 7c**) and did not bind ClpP in pull-down assays containing ATPγS, ATP or ADP (**Fig. 7a**). In addition, ClpX R370K did not show detectable binding to a fluorescent ssrA peptide in the presence of ATPγS (K_d > 20 μM; wild-type $K_d \cong$ 3 μM; ref. 36), did not unfold GFP-ssrA and did not degrade GFP-ssrA when ClpP was present (data not shown). These results suggest that interactions between Arg370 and bound ATP are required to stabilize a ClpX conformation that has a high affinity for both ClpP and ssrA-tagged substrates.

To determine whether the mutant R370K and wild-type subunits coassemble, we titrated increasing quantities of ClpX R370K against a fixed quantity of wild-type ClpX and excess ClpP and assayed degradation of GFP-ssrA (**Fig. 7d**). Addition of the mutant in 12-fold excess caused nearly complete inhibition. We also observed inhibition by ClpX R370K of ClpXP degradation of denatured CM-titin-ssrA and of ClpX unfolding of GFP-ssrA (data not shown). Hence, mixed hexamers with one wild-type dimer and two ClpX R370K dimers must be inactive in these assays. The best fit of the inhibition data (**Fig. 7d**) was obtained from a model in which the 2:1 and 1:2 mixed hexamers were both inactive, and wild-type dimers had a three-fold preference for assembling with themselves rather than with mutant dimers. Untagged ClpP bound Ni^{2+}-NTA resin after incubation with His_6-ClpX R370K, untagged wild-type ClpX and ATPγS (**Fig. 7d**, inset). This result demonstrates that ClpX R370K and wild-type subunits coassemble and shows that at least one species of mixed hexamer can bind ClpP. With a six-fold excess of ClpX R370K, the ATPase activity of wild-type ClpX was reduced by only ~30% (data not shown). Hence, mixed hexamers containing wild-type and R370K subunits retain some ATPase activity but cannot bind or process protein substrates.

DISCUSSION

The studies presented here provide strong evidence for functional communication between ClpX and ClpP during the processing and degradation of protein substrates. For example, ClpP affinity improved during substrate processing by ClpX. Like other molecular machines, ClpX must undergo a conformational change during the ATPase cycle. If the ATP and ADP conformations of ClpX have different affinities for ClpP, as suggested by our results, then alterations in the ATPase rate and thus the time spent in each stage of the cycle would modulate ClpX-ClpP affinity (**Fig. 8**). Earlier studies have shown that the ATPase rate of ClpXP is roughly four-fold higher during translocation than denaturation of titin-ssrA substrates[35]. Hence, the ATP-bound states would be more highly populated when ClpX is engaged in denaturing native titin-ssrA than during translocation (**Fig. 8**). This model explains why the apparent affinity of the ClpX-ClpP interaction correlates with the degradation rates of different titin-ssrA substrates and with the ATPase rates during the processing of these substrates.

ClpX bound much more tightly when the active site serines of ClpP were acylated by reaction with DFP. Previous studies also suggest that ClpA binds more strongly to DFP-ClpP than to the unmodified enzyme[41]. Because the DFP-modified residues are located within the degradation chamber of ClpP[7], they cannot affect interactions with the ATPases directly. We suggest that DFP modification of the ClpP active sites lowers the energy required for a conformational change that occurs upon binding to ClpX. In the model (**Fig. 8**), this would increase ClpX-ClpP affinity by allowing more of the interaction energy to drive the binding reaction. Even though the ClpP and HslV peptidases have unrelated structures and active site architectures, ClpXP and HslUV both have mechanisms that allow communication between the ATPase active sites and the peptidase active sites. This functional conservation, even in the absence of structural conservation, emphasizes the importance of communication between the processing and protease compartments of these energy-dependent proteases during protein degradation.

The IGF loop of *E. coli* ClpX seems to be the major determinant of ClpP binding, and related peptide motifs are found in all of the AAA^+ ATPases that collaborate with ClpP homologs[26]. In the crystal structure of *H. pylori* ClpX[29], a homologous LGF tripeptide (yellow in **Fig. 1**) sits at the tip of a surface loop that extends away from the protease-proximal surface. Alignment of the symmetry axes of the ClpX and ClpP rings positions these tripeptides from the ClpX hexamer near hydrophobic clefts on the surface of a ClpP ring[26] (**Fig. 1b**). In each ClpX subunit[29], the IGF LGF loop is preceded by a short α-helix that connects directly to the sensor I portion of the binding site for ATP or ADP. In ClpA, the corresponding loop is disordered but is also

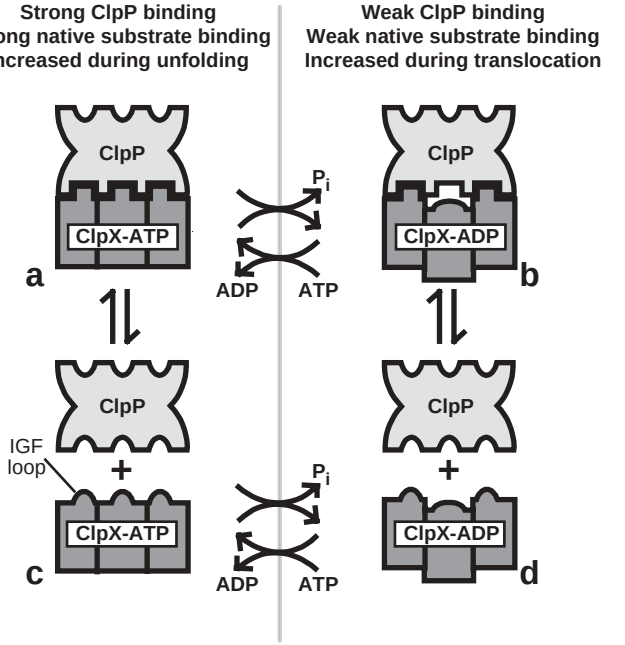

Figure 8 Model for the interaction of ClpX and ClpP. Cartoon depiction of ClpX and ClpXP in ATP-bound and ADP-bound states. ClpX-ATP binds ClpP more strongly than ClpX-ADP. The depression of the ATPase activity of ClpX upon ClpP binding occurs because of conformation changes or restraints in the IGF loops. Bound native protein substrates (data not shown) affect the ATPase activity of ClpX independently and increase apparent ClpP affinity by binding preferentially to the ATP-bound enzymes. During the processing of protein substrates (not shown), the ATP-bound enzymes are stabilized during denaturation, whereas the ADP-bound enzymes are more highly populated during translocation. ClpX R370K is trapped in the ADP conformation, even when ATP is bound, explaining its inability to bind ClpP or native substrates. DFP modification of the active sites of ClpP stabilizes the ClpX-bound conformation of the peptidase relative to its free conformation.

connected to the sensor I portion of an active site for ATP hydrolysis[28]. As illustrated in the model (**Fig. 8**), changes in the conformation of the IGF loops upon ClpP binding and/or changes in the number of loops that contact ClpP could regulate ClpX-ClpP affinity in a manner dependent on the nucleotide state of ClpX. ClpX and ClpA crystallize not as ring hexamers but in 'lock-washer' conformations, in which subunits are related by a screw axis[28,29]. If the ADP states of these ATPases resembled this lock-washer conformation, then only a subset of the IGF loops would be positioned to contact a ClpP ring.

Our results suggest that one role of the sensor II helix in ClpX is to link ATP binding with structural changes required for the 'ATP' conformation. The ClpX R370K sensor II mutant binds but cannot hydrolyze ATP, has low affinity for ClpP and ssrA-tagged substrates, and has no GFP-ssrA unfolding or degradation activity. In terms of the model (**Fig. 8**), we propose that the defects of this mutant arise because it is trapped in the 'ADP' state irrespective of the identity of the bound nucleotide. Failure to adopt the ATP conformation would explain the absence of ATPase activity for the R370K mutant as well as its inability to bind strongly to ssrA-tagged substrates or to ClpP. The protein-processing defects of this mutant are easily explained by the ssrA-tag binding and ATP hydrolysis defects. On the basis of the *H. pylori* ClpX structure[29], the Arg370 side chain is positioned to contact bound ATP, and these interactions could be needed to adopt or stabilize the ATP conformation. The inactivity in protein processing of ClpX hexamers containing mixtures of R370K and wild-type dimers suggests that the conformations and/or ATPase activities of different subunits must be coordinated for this function. ATPγS, which is hydrolyzed slowly, does not support unfolding of stable protein substrates by wild-type ClpX[40], again suggesting that proper coordination of ATP hydrolysis by different ClpX subunits is important.

Mutations at the C-terminal end of the sensor II helix disrupt packing between subunits in the hexamer and result in ClpX enzymes that bind but fail to unfold ssrA-tagged substrates[39]. ClpP binding suppresses the substrate-processing defects of several of these sensor II mutants, including ClpX D382K. ClpP binding to ClpX D382K is similar to wild-type ClpX in the absence of protein substrates but becomes much weaker in the presence of native substrates. These results suggest that when ClpX D382K binds to and attempts to unfold a native ssrA-tagged substrate, it becomes trapped in a conformation that is inactive for protein unfolding and binds ClpP poorly. Hence, maintenance of proper contacts between subunits within ClpX seems to be essential for both substrate unfolding and strong ClpP interactions. We propose that subunit-subunit contacts mediated by Asp382 and surrounding residues in *E. coli* ClpX resist tension generated when the enzyme applies an unfolding force to a native substrate. Such tension would be a natural consequence of the unfolding force applied to a protein substrate, because this process must create an equal and opposite force. If this tension results in quaternary distortions of ClpX D382K, then ClpP binding could stabilize the active ATPase conformation, allowing it to resist distortion and use the energy of ATP hydrolysis for productive conformational changes that drive substrate unfolding.

What function is served by communication between ClpX and ClpP during substrate processing? The total $ClpX_6$ concentration in *E. coli* is estimated to be within three-fold of K_{app} for the ClpX-ClpP interaction in the absence of substrate. Thus, substrate binding to free ClpX hexamers would be expected to drive assembly of ClpXP complexes. Because ClpP in the cell can associate with either ClpX or ClpA, this tightening could provide a mechanism by which ClpP is distributed according to the relative prevalence of substrates for one ATPase or the other. Communication may also facilitate translocation of denatured substrates from ClpX to ClpP by coordinating changes in the diameters of the ATPase processing pore and the peptidase entry portal. This coordination of conformational changes could allow efficient substrate transfer during the power stroke associated with each cycle of ATP hydrolysis and prevent slippage or dissociation during the recovery phase. Coordination also may be required to allow efficient release of cleaved peptides from the degradation chamber at the same time that uncleaved polypeptide chains enter the chamber. Finally, when ClpX hexamers are docked with both peptidase rings of ClpP, a situation expected when ClpX is in excess over ClpP, translocation seems to occur exclusively from one ClpX hexamer rather than simultaneously from both hexamers[42]. Communication between ClpX and ClpP would obviously be critical for regulating substrate traffic under these circumstances.

METHODS

Solutions. Buffer A: 43 mM HEPES-KOH, pH 7.6, 8.5 mM Tris-HCl, pH 8.0, 142 mM KCl, 15% (v/v) glycerol, 1.1 mM DTT, 5.4 mM $MgCl_2$, 420 μM EDTA, 36 μM $ZnSO_4$, 36 μM ATP, 0.032% (v/v) NP-40 and 0.004% (v/v) Triton X-100. Buffer B: 35 mM HEPES-KOH, pH 7.6, 4.4 mM Tris-HCl, pH 7.6, 1.5 mM Tris-HCl, pH 8.0, 95 mM KCl, 14% (v/v) glycerol, 660 μM DTT, 7.4 mM $MgCl_2$, 85 μM EDTA, 19 μM $ZnSO_4$, 19 μM ATP, 0.16% (v/v) NP-40 and 0.002% (v/v) Triton X-100. Buffer L: 50 mM Tris-HCl, pH 7.6, 10% (v/v) glycerol, 1 mM DTT and 0.5 mM EDTA. Buffer M: 47 mM Tris-HCl, pH 7.6, 284 mM KCl, 9.5% (v/v) glycerol, 4.7 mM DTT, 95 μM $MgCl_2$ and 10 mM EDTA. Buffer N: 50 mM sodium phosphate, pH 8.0, 300 mM NaCl and 250 mM imidazole.

Buffer S: 50 mM Tris-HCl, pH 8.0, 300 mM KCl, 10% (v/v) glycerol, 3 mM DTT and 10 mM $MgCl_2$. ATP mix I: 5 mM ATP, 16 mM creatine phosphate and 0.32 mg ml^{-1} creatine phosphokinase. ATP mix III: 2.5 mM ATP, 1 mM NADH, 7.5 mM phosphoenolpyruvate, 0.05 mg ml^{-1} pyruvate kinase and 0.025 mg ml^{-1} lactate dehydrogenase.

Strains, plasmids and proteins. *E. coli* strain CF150, an X90 derivative, in which a *cat* gene replaces the *clpP*, *clpX* and *lon* genes, was provided by C. Farrell (MIT). A plasmid expressing His_6-ClpX R370K (pSJ62) was produced using overlap extension mutagenesis[39]. A plasmid expressing ClpX loopless (pGH003) was constructed from pET-3a-ClpX[43] by PCR. In ClpX loopless, a GSGSG sequence replaces wild-type residues 264–278. The synthetic peptide sequence containing the IGF loop (underlined) of ClpX was fluorescein-NH-KKGRYTGSGIGFGATVKAK-$CONH_2$.

ClpX loopless and wild-type ClpX were purified as described[40], as were GFP-ssrA and His_6-tagged variants of ClpP, ClpX and titin-I27-ssrA[31,35,39]. ^{35}S-labeled titin-ssrA variants were gifts from J. Kenniston (MIT), and SspB was provided by D. Wah (MIT). His_6-ClpP S97A was purified from *E. coli* strain CF150 containing pYK162 (ref. 38) using a described protocol[31] with modifications. After Mono Q chromatography, ClpP S97A fractions were applied to a HiPrep 16/60 Sephacryl S-300HR column (Amersham Biosciences) equilibrated in buffer S. Purified protein fractions were pooled and stored at –80 °C. Carboxymethylation of titin-ssrA variants and acylation of ClpP variants with DFP were done as described[31,35]. Chemically modified proteins were dialyzed extensively before use.

E. coli ClpP was purified using a described protocol[44] with modifications. Cells were resuspended in 3 ml of buffer L plus 150 mM KCl for each gram of cells, lysed by French press and centrifuged at 15,000 r.p.m. 23,222*g* in a SA-600 rotor for 60 min. The supernatant was filtered, ammonium sulfate was added to 30% (w/v) saturation and the supernatant containing ClpP was retained after centrifugation. Ammonium sulfate was added to this supernatant to 60% (w/v) saturation, and the pellet containing ClpP was recovered by centrifugation. The pellet was resuspended, desalted into buffer L plus 150 mM KCl using a PD-10 column (Amersham Biosciences) and loaded onto a HiLoad 16/10 Q Sepharose HP column (Amersham Biosciences) equilibrated in buffer L with 150 mM KCl. ClpP was eluted with a 200-ml linear gradient from 150 mM to 400 mM KCl in buffer L and concentrated by ammonium sulfate precipitation (60% (w/v) saturation). The pellet containing ClpP was resuspended, desalted into buffer L plus 100 mM KCl and loaded onto a HiPrep 16/60 Sephacryl S-300HR column equilibrated in this buffer. Fractions containing purified ClpP were pooled, concentrated by chromatography on a HiLoad 16/10 Q Sepharose HP column and stored in aliquots at –80 °C.

Nucleotide hydrolysis and binding assays. ATP hydrolysis by ClpX in buffer A was measured at 30 °C using a coupled assay[26]. ClpX and ClpP were incubated for 2 min before addition of substrate and/or ATP mix III. Except where noted, 50 nM $ClpX_6$ was used for all assays. K_{app} values for ClpX-ClpP binding were determined by plotting ATPase rates (R_{obs}) versus the total ClpP concentration (*PT*) and fitting to equation (1):

$$R_{obs}=R_0\pm\{R_1[(XT+PT+K_{app})-((XT+PT+K_{app})^2-4XT\times PT)^{0.5}]\}/(2XT) \quad (1)$$

where R_0 is the ATPase rate without ClpP, R_1 is the ATPase rate with saturating ClpP and *XT* is the total ClpX concentration[45]. Mant-ADP or mant-ATP binding to ClpX R370K was assayed at 4 °C in buffer M[40].

Substrate unfolding, degradation and binding assays. GFP-ssrA unfolding or degradation[31] was carried out in buffer B plus ATP mix I at 30 °C. In mixing experiments with ClpX R370K, wild-type and mutant ClpX were first incubated for 5 min at 30 °C, ClpP and ATP mix I were added and GFP-ssrA was added 2 min later to start the reaction. Degradation of ^{35}S-labeled titin-ssrA substrates was assayed by TCA-soluble peptide release[33,35]. For ClpXP degradation of titin-ssrA substrates at saturating concentrations, the slow steps are denaturation (k_{den}) and translocation (k_{trans}), with $1/k_{deg} = 1/k_{den} + 1/k_{trans}$ and $\tau_{deg} = \tau_{den} + \tau_{trans}$ (ref. 35). K_{app} for the ClpX-ClpP interaction during substrate processing can be expressed as $(\tau_{den}/\tau_{deg})K_{app}^{den} + (\tau_{trans}/\tau_{deg})K_{app}^{trans}$. The value of k_{trans} for different titin-ssrA substrates is essentially constant (4.3 min^{-1}). Substitution of $\tau_{deg} - \tau_{trans}$ for τ_{den} and rearrangement of terms yields the linear equation (2):

$$K_{app} = \tau_{trans}(K_{app}^{trans} - K_{app}^{den})k_{deg} + K_{app}^{den} \quad (2)$$

The general equation for inhibition by mixed hexamer formation between active and inactive dimers of ClpX is

$$A = (1 + 3A_{21}BR + 3A_{12}B^2R^2) / (1 + BR)^2 \quad (3)$$

where *A* is the fractional activity of fully active hexamers, A_{21} is the fractional activity of a hexamer with two active and one inactive dimer, A_{12} is the activity of a hexamer with one active and two inactive dimers, *R* is the ratio of total inactive to total active subunits and *B* is the mixing bias. $B = 1$ indicates unbiased mixing of active and inactive dimers; $B < 1$ indicates a preference of active dimers to associate with other active dimers rather than inactive dimers. If three active dimers are required for activity, equation (3) simplifies to

$$A = (1 + BR)^{-2} \quad (4)$$

Binding of a fluorescent ssrA peptide to ClpX or ClpX R370K was assayed by changes in fluorescence anisotropy as described[36].

Pull-down and ternary complex assays. ClpXP pull-down assays were done using a published protocol with modifications[26]. Each reaction (30 µl) contained 300 nM His_6-$ClpX_6$ (wild type or R370K) and 300 nM untagged $ClpP_{14}$. Some reactions also contained 300 nM untagged wild-type $ClpX_6$. Also present during initial complex formation and in washes after binding to Ni^{2+}-NTA agarose was 3 mM nucleotide (ATPγS, ATP or ADP) . Protein was eluted in 30 µl buffer N and subjected to SDS-PAGE. Gels were stained with Sypro Orange (Molecular Probes) and visualized using a FluorImager 595 (Molecular Dynamics). Assays for ternary complexes of ClpX, SspB and GFP-ssrA were done by gel-filtration chromatography on a Superdex 200 column (Amersham Biosciences) as described[36].

ACKNOWLEDGMENTS

We thank S. Boyd, R. Burton, E. Courtenay, C. Farrell, J. Flynn, R. Grant, J. Kenniston, I. Levchenko, S. Siddiqui and D. Wah for discussion and materials, R. Horvitz and J. King for use of equipment and D. Kim and K. Kim (Sungkyunkwan University School of Medicine, Korea) for the ClpX hexamer coordinates. This work was supported by grants from the US National Institutes of Health and the Howard Hughes Medical Institute (HHMI). T. Baker is an employee of HHMI.

COMPETING INTERESTS STATEMENT

The authors declare that they have no competing financial interests.

Received 28 November 2003; accepted 3 March 2004
Published online at http://www.nature.com/natstructmolbiol/

1. Ogura, T. & Wilkinson, A.J. AAA+ superfamily ATPases: common structure—diverse function. *Genes Cells* **6**, 575–597 (2001).
2. Glickman, M.H. *et al.* A subcomplex of the proteasome regulatory particle required for ubiquitin-conjugate degradation and related to the COP9-signalosome and eIF3. *Cell* **94**, 615–623 (1998).
3. Gottesman, S., Wickner, S. & Maurizi, M.R. Protein quality control: triage by chaperones and proteases. *Genes Dev.* **11**, 815–823 (1997).
4. Gottesman, S., Maurizi, M.R. & Wickner, S. Regulatory subunits of energy-dependent proteases. *Cell* **91**, 435–438 (1997).
5. Bochtler, M., Ditzel, L., Groll, M. & Huber, R. Crystal structure of heat shock locus V (HslV) from *Escherichia coli*. *Proc. Natl. Acad. Sci. USA* **94**, 6070–6074 (1997).
6. Groll, M. *et al.* Structure of 20S proteasome from yeast at 2.4 Å resolution. *Nature* **386**, 463–471 (1997).
7. Wang, J., Hartling, J.A. & Flanagan, J.M. The structure of ClpP at 2.3 Å resolution suggests a model for ATP-dependent proteolysis. *Cell* **91**, 447–456 (1997).
8. Wang, J., Hartling, J.A. & Flanagan, J.M. Crystal structure determination of *Escherichia coli* ClpP starting from an EM-derived mask. *J. Struct. Biol.* **124**, 151–163 (1998).
9. Bochtler, M. *et al.* The structures of HslU and the ATP-dependent protease HslU-HslV. *Nature* **403**, 800–805 (2000).
10. Groll, M. *et al.* A gated channel into the proteasome core particle. *Nat. Struct. Biol.* **7**, 1062–1067 (2000).
11. Sousa, M.C. *et al.* Crystal and solution structures of an HslUV protease-chaperone complex. *Cell* **103**, 633–643 (2000).

12. Whitby, F.G. *et al.* Structural basis for the activation of 20S proteasomes by 11S regulators. *Nature* **408**, 115–120 (2000).
13. Wang, J. *et al.* Crystal structures of the HslVU peptidase-ATPase complex reveal an ATP-dependent proteolysis mechanism. *Structure* **9**, 177–184 (2001).
14. Sousa, M.C. & McKay, D.B. Structure of *Haemophilus influenzae* HslV protein at 1.9 Å resolution, revealing a cation-binding site near the catalytic site. *Acta Crystallogr. D* **57**, 1950–1954 (2001).
15. Guenther, B., Onrust, R., Sali, A., O'Donnell, M. & Kuriyan, J. Crystal structure of the δ' subunit of the clamp-loader complex of *E. coli* DNA polymerase III. *Cell* **91**, 335–345 (1997).
16. Neuwald, A.F., Aravind, L., Spouge, J.L. & Koonin, E.V. AAA+: a class of chaperone-like ATPases associated with the assembly, operation, and disassembly of protein complexes. *Genome Res.* **9**, 27–43 (1999).
17. Wang, J. *et al.* Nucleotide-dependent conformational changes in a protease-associated ATPase HslU. *Structure* **9**, 1107–1116 (2001).
18. Sousa, M.C., Kessler, B.M., Overkleeft, H.S. & McKay, D.B. Crystal structure of HslUV complexed with a vinyl sulfone inhibitor: corroboration of a proposed mechanism of allosteric activation of HslV by HslU. *J. Mol. Biol.* **318**, 779–785 (2002).
19. Yoo, S.J. *et al.* Purification and characterization of the heat shock proteins HslV and HslU that form a new ATP-dependent protease in *Escherichia coli*. *J. Biol. Chem.* **271**, 14035–14040 (1996).
20. Seol, J.H. *et al.* The heat-shock protein HslVU from *Escherichia coli* is a protein-activated ATPase as well as an ATP-dependent proteinase. *Eur. J. Biochem.* **247**, 1143–1150 (1997).
21. Ramachandran, R., Hartmann, C., Song, H.K., Huber, R. & Bochtler, M. Functional interactions of HslV (ClpQ) with the ATPase HslU (ClpY). *Proc. Natl. Acad. Sci. USA* **99**, 7396–7401 (2002).
22. Seong, I.S. *et al.* The C-terminal tails of HslU ATPase act as a molecular switch for activation of HslV peptidase. *J. Biol. Chem.* **277**, 25976–25982 (2002).
23. Grimaud, R., Kessel, M., Beuron, F., Steven, A.C. & Maurizi, M.R. Enzymatic and structural similarities between the *Escherichia coli* ATP-dependent proteases, ClpXP and ClpAP. *J. Biol. Chem.* **273**, 12476–12481 (1998).
24. Beuron, F. *et al.* At sixes and sevens: characterization of the symmetry mismatch of the ClpAP chaperone-assisted protease. *J. Struct. Biol.* **123**, 248–259 (1998).
25. Ortega, J., Singh, S.K., Ishikawa, T., Maurizi, M.R. & Steven, A.C. Visualization of substrate binding and translocation by the ATP-dependent protease, ClpXP. *Mol. Cell* **6**, 1515–1521 (2000).
26. Kim, Y.I. *et al.* Molecular determinants of complex formation between Clp/Hsp100 ATPases and the ClpP peptidase. *Nat. Struct. Biol.* **8**, 230–233 (2001).
27. Singh, S.K. *et al.* Functional domains of the ClpA and ClpX molecular chaperones identified by limited proteolysis and deletion analysis. *J. Biol. Chem.* **276**, 29420–29429 (2001).
28. Guo, F., Maurizi, M.R., Esser, L. & Xia, D. Crystal structure of ClpA, an Hsp100 chaperone and regulator of ClpAP protease. *J. Biol. Chem.* **277**, 46743–46752 (2002).
29. Kim, D.Y. & Kim, K.K. Crystal structure of ClpX molecular chaperone from *Helicobacter pylori*. *J. Biol. Chem.* **278**, 50664–50670 (2003).
30. Thompson, M.W., Singh, S.K. & Maurizi, M.R. Processive degradation of proteins by the ATP-dependent Clp protease from *Escherichia coli*. Requirement for the multiple array of active sites in ClpP but not ATP hydrolysis. *J. Biol. Chem.* **269**, 18209–18215 (1994).
31. Kim, Y.I., Burton, R.E., Burton, B.M., Sauer, R.T. & Baker, T.A. Dynamics of substrate denaturation and translocation by the ClpXP degradation machine. *Mol. Cell* **5**, 639–648 (2000).
32. Hwang, B.J., Woo, K.M., Goldberg, A.L. & Chung, C.H. Protease Ti, a new ATP-dependent protease in *Escherichia coli*, contains protein-activated ATPase and proteolytic functions in distinct subunits. *J. Biol. Chem.* **263**, 8727–8734 (1988).
33. Gottesman, S., Roche, E., Zhou, Y. & Sauer, R.T. The ClpXP and ClpAP proteases degrade proteins with carboxy-terminal peptide tails added by the SsrA-tagging system. *Genes Dev.* **12**, 1338–1347 (1998).
34. Singh, S.K., Grimaud, R., Hoskins, J.R., Wickner, S. & Maurizi, M.R. Unfolding and internalization of proteins by the ATP-dependent proteases ClpXP and ClpAP. *Proc. Natl. Acad. Sci. USA* **97**, 8898–8903 (2000).
35. Kenniston, J.A., Baker, T.A., Fernandez, J.M. & Sauer, R.T. Linkage between ATP consumption and mechanical unfolding during the protein processing reactions of an AAA+ degradation machine. *Cell* **114**, 511–520 (2003).
36. Wah, D.A., Levchenko, I., Baker, T.A. & Sauer, R.T. Characterization of a specificity factor for an AAA+ ATPase. Assembly of SspB dimers with ssrA-tagged proteins and the ClpX hexamer. *Chem. Biol.* **9**, 1237–1245 (2002).
37. Wojtyra, U.A., Thibault, G., Tuite, A. & Houry, W.A. The N-terminal zinc binding domain of ClpX is a dimerization domain that modulates the chaperone function. *J. Biol. Chem.* **278**, 48981–48990 (2003).
38. Flynn, J.M., Neher, S.B., Kim, Y.I., Sauer, R.T. & Baker, T.A. Proteomic discovery of cellular substrates of the ClpXP protease reveals five classes of ClpX-recognition signals. *Mol. Cell* **11**, 671–683 (2003).
39. Joshi, S.A., Baker, T.A. & Sauer, R.T. C-terminal domain mutations in ClpX uncouple substrate binding from an engagement step required for unfolding. *Mol. Microbiol.* **48**, 67–76 (2003).
40. Burton, R.E., Baker, T.A. & Sauer, R.T. Energy-dependent degradation: linkage between ClpX-catalyzed nucleotide hydrolysis and protein-substrate processing. *Protein Sci.* **12**, 893–902 (2003).
41. Singh, S.K., Guo, F. & Maurizi, M.R. ClpA and ClpP remain associated during multiple rounds of ATP-dependent protein degradation by ClpAP protease. *Biochemistry* **38**, 14906–14915 (1999).
42. Ortega, J., Lee, H.S., Maurizi, M.R. & Steven, A.C. Alternating translocation of protein substrates from both ends of ClpXP protease. *EMBO J.* **21**, 4938–4949 (2002).
43. Levchenko, I., Luo, L. & Baker, T.A. Disassembly of the Mu transposase tetramer by the ClpX chaperone. *Genes Dev.* **9**, 2399–2408 (1995).
44. Levchenko, I., Yamauchi, M. & Baker, T.A. ClpX and MuB interact with overlapping regions of Mu transposase: implications for control of the transposition pathway. *Genes Dev.* **11**, 1561–1572 (1997).
45. Segel, I.H. Enzyme Kinetics: Behavior and Analysis of Rapid Equilibrium and Steady-State Enzyme Systems (Wiley Classics Library edn) 72–74 (Wiley, New York, 1993).
46. Karon, B.S., Mahaney, J.E. & Thomas, D.D. Halothane and cyclopiazonic acid modulate Ca-ATPase oligomeric state and function in sarcoplasmic reticulum. *Biochemistry* **33**, 13928–13937 (1994).